Observation of Dual Room Temperature Fluorescence-Phosphorescence in Air, in the Crystal Form of a Thianthrene Derivative

Piotr Pander,[†] *Agnieszka Swist,*[‡] *Roman Turczyn,*[∞] *Stephanie Pouget,*[⊥] *David Djurado,*[⊥] *Algirdas Lazauskas,*[§] *Ramin Pashazadeh,*[∥] *Juozas V. Grazulevicius,*[∥] *Radoslaw Motyka,*[∞] *Anastasia Klimash,*[⁂] *Peter Skabara,*[⁂] *Przemyslaw Data,*[†,∞] *Jadwiga Soloducho,*[‡] *Fernando B. Dias* [*,†]

[†] University of Durham, Department of Physics, South Road, Durham, DH1 3LE, United Kingdom

[‡] Wroclaw University of Technology, Faculty of Chemistry, Wybrzeze Wyspianskiego 27, 50-370 Wroclaw, Poland

[§] Kaunas University of Technology, Institute of Materials Science, K. Baršausko Str. 59, LT-51423 Kaunas, Lithuania

[∥] Kaunas University of Technology, Department of Polymer Chemistry and Technology, Radvilenu pl. 19, LT-50254 Kaunas, Lithuania

[∞] Faculty of Chemistry, Silesian University of Technology, M. Strzody 9, 44-100 Gliwice, Poland

[⊥] Université Grenoble Alpes, CNRS, INAC/ SyMMES/MEM, CEA Grenoble, 17 rue des Martyrs – 38054 – Grenoble – cedex 9, France

[⁂] University of Glasgow, School of Chemistry, Joseph Black Building, University Avenue, Glasgow G12 8QQ, United Kingdom

ABSTRACT

Thianthrenes have been nearly forgotten as phosphors in recent years, but are now coming back, showing their strong potential in luminescent applications. Here, we present a comprehensive photophysical study of a carbazolyl derivative of thianthrene in different matrices and environments. The diffusion of oxygen is slowed down in the rigid environment of thianthrene organic crystals suppressing their phosphorescence quenching, as well as triplet-triplet annihilation. This facilitates the observation of simultaneous fluorescence and phosphorescence emissions at room temperature, in air, giving origin to strong white luminescence. Moreover, the color coordinates of the dual fluorescence-phosphorescence white emission, which is observed only in rigid amorphous media and in crystals, can be tuned.

1. INTRODUCTION

Thianthrenes have attracted attention due to their high triplet formation yield and strong phosphorescent properties in the solid state.[1,2] Spin-orbit coupling interactions induced by the nπ* transitions and the heavy-atom effect caused by the presence of sulfur, lead to its remarkable phosphorescent properties.[3–7] As a result, thianthrene and its analogs are mediocre photoluminescence emitters in conditions where the triplet state is effectively quenched by the surrounding environment, i.e. in solution or in the presence of oxygen.[8,9] Interestingly, some authors have previously described that diquinoline derivatives are relatively highly-luminescent in aerated solutions, despite being closely related with thianthrene or phenothiazine bearing one or two single sulfur bridges.[10] This underlines the potential role of fine structural tuning of the electronic states to optimize the contribution of the sulfur atoms in order to promote efficient spin-orbit coupling and triplet harvesting to the luminescence mechanism. The key to facilitate the observation of phosphorescence at room temperature is to remove the causes of luminescence quenching, i.e. reducing the non-radiative decay rate and removing or reducing the effects of quenching caused by oxygen. As it has been shown in previous works,[1,6,11–13] the non-radiative decay rate can be suppressed when the compound is dispersed in a rigid solid matrix. This can be either a polymeric or small molecule host. However, even in a rigid host, when the rate of oxygen diffusion is sufficiently fast, no phosphorescence is observed while the sample is surrounded by air. This effect is often used to confirm the triplet origin of the phosphorescence emission.[14,15] On the other hand, if the oxygen diffusion is effectively reduced in the host material, such as it happens in β-estradiol,[13] or in molecular crystals,[16] strong room temperature phosphorescence (RTP) in ambient conditions may be observed. The only requirements for a RTP host is thus to create conditions for the slow non-radiative decay of triplet states and ensure low oxygen permeability at a certain temperature. However, when the natural decay time of an emitter is relatively short, then the rigidity or oxygen permeability of the host become less important.[17]

It is also worth to note that frequently due to the presence of an effectively large singlet-triplet energy gap in most RTP emitters, thermally activated delayed fluorescence (TADF) is not observed in such systems.[7,14,18,19] Finally, the combination of fluorescence and phosphorescence in adequate proportion and color (i.e. blue + yellow/orange) can result in white photoluminescence.[20] Therefore, dual fluorescence-phosphorescence can for example be interesting to the development of advanced anti-counterfeiting inks, which exploit the change in emission color of the ink under UV illumination and after the illumination has been switched off.[21]

In this work a thianthrene derivative (**Figure 1 a**) showing dual fluorescence-phosphorescence properties in the presence of air in the solid form is investigated. The compound is similar to thianthrene, which is also used for comparison, and shows room temperature phosphorescence emission in the crystal form, as a result of aggregation enhanced emission. Interestingly, the effect of crystallization can also be observed in blend films with the popular 1,3-bis(N-carbazolyl)benzene (mCP) OLED host. The film obtained by slow crystallization of the blend at room temperature shows remarkable phosphorescent properties, with a 30% luminescence quantum yield, and 60-70% contribution to the total photoluminescence due to the phosphorescence. Remarkably, this observed in the presence of air and at room temperature.

2. RESULTS AND DISCUSSION

2.1 Photoluminescence and absorption spectra in solution

The absorption spectrum of **CbTT** (**Figure 1 b**) clearly shows the contribution from both building units: the thianthrene and carbazole. Very characteristic absorption bands peaking at λ_{max} = 337 nm and λ_{max} = 292 nm are originated from carbazole, and can be found in several carbazole derivatives.[1,22] On the other hand, the absorption band at λ_{max} = 258 nm is clearly originating from thianthrene. This situation is a strong indication that thianthrene and carbazole are not well conjugated. A previous study[1] has shown that the $\pi\pi^*$ absorption band in thianthrene (λ_{max} = 258 nm) shifts when its conjugation is extended, while in **CbTT** this does not happen. Therefore, this observation confirms that no strong conjugation occurs in **CbTT** between the carbazole and the thianthrene moieties. It is however expected, that similarly to the other molecules with *N*-carbazolyl substituent, the dihedral angle between carbazole and thianthrene phenyl ring will be close to 60°, rather than the 90°expected for a perfect orthogonal orientation.[22–24] This is further confirmed by ground state geometry calculations performed using density functional theory (**Figure S13**, **S14**), indicating the dihedral angle between carbazole and phenyl ring equals 53.1°. Also, the HOMO is localised mostly on the carbazole moiety, suggesting a stronger electron-donating property of this unit relatively to thianthrene. This is consistent with the electrochemical characteristics of the molecule (**Figure S12**) indicating non-reversibility[25–28] of the oxidation process as typically for carbazole.[22,29] HOMO located on the thianthrene would result in a reversible oxidation cycle.[30,31] LUMO is on the other hand situated on the thianthrene moiety.

CbTT emits weak blue fluorescence in methylcyclohexane (MCH) solution. The emission spectrum is given in **Figure 1b** and the fluorescence quantum yield in **Table 1**. This is similar to pure thianthrene. However, the emission of **CbTT** appears to be much stronger than that of thianthrene due to the absorption bands in the range of 270-350 nm showing a higher molar absorption coefficient and oscillator strength in **CbTT** that is not observed in thianthrene. The fluorescence of **CbTT** decays with 9.4 ± 0.4 ns lifetime in degassed methylcyclohexane (MCH) solution, with almost no effect of oxygen on its intensity. As fluorescence occurs from the singlet state the fast radiative decay, this observation indicates that the singlet state decays radiatively much faster than it is quenched by oxygen molecules. However, no phosphorescence nor delayed fluorescence is observed in a degassed solution. Showing the triplet state population is strongly quenched in solution even in the absence of oxygen, probably due to collisions with solvent molecules. This is consistent with the common experimental observations of phosporescence quenching in liquid medium for many other molecules.

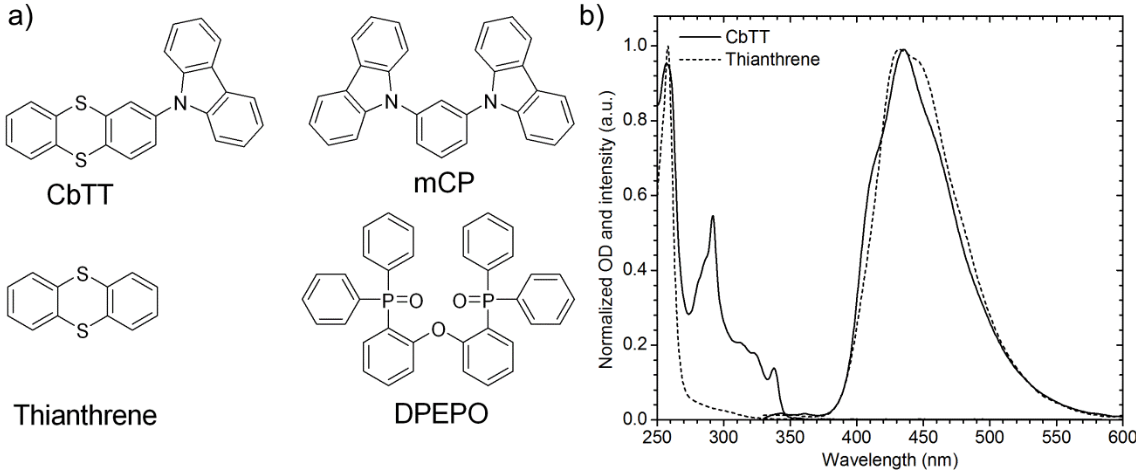

Figure 1. a) Molecular structures of the compounds studied in this work. b) Photoluminescence and absorption spectra of **CbTT** (10^{-5} M) and **thianthrene** (5×10^{-5} M) in methylcyclohexane.

2.2 Film and powder XRD study: crystallization vs. photoluminescence color

The rigidity in the crystal form is of vital importance for observation of **CbTT** phosphorescence in ambient conditions (see later in the text). For this reason, XRD studies were used to characterize the crystal form, and differentiate from conditions where **CbTT** is on its amorphous form. Both powders of **CbTT** and thianthrene analyzed in this paper are clearly in their crystal forms (**Figure 2 a**). However, the fresh films of **CbTT** in **mCP** and **DPEPO** (bis[2-(diphenylphosphino)phenyl]ether oxide), both with 10% w/w doping concentration, see **Figure 1 a**, are amorphous. However, the film doped in **mCP** crystallizes over time at room temperature. This film is identified as "old". No crystallization was observed in the **CbTT** film in **DPEPO** host, either over time at room temperature or upon heating and cooling cycles. It is worth to note that the diffraction pattern of the crystal **CbTT**/**mCP** film does not contain diffraction peaks of single materials in their powder form. This is a strong indication that the blend **CbTT**/**mCP** forms a co-crystal. It is further shown in the photophysical study that the luminescent properties of **CbTT** are clearly different in the co-crystal, single crystal and when doped in zeonex. Such behavior agrees with the conclusions from the XRD study.

All crystalline samples show relatively balanced dual fluorescence-phosphorescence emission, thus creating white photoluminescence (**Figure 2 b**). The **thianthrene** crystal shows white-greenish photoluminescence in air, CIE (0.32, 0.43), and the **CbTT** crystal shows warm white luminescence,[32,33] CIE (0.29, 0.31), whereas the crystallized film (old) of **CbTT** in **mCP** shows cool white emission,[32,33] CIE (0.36, 0.37). In contrast, the amorphous film (fresh) of **CbTT** in **mCP** emits weak sky-blue fluorescence, CIE (0.18, 0.16), all in the presence of air. The photoluminescent properties of the blends and crystals are described later in the text.

The results show the effect of rigidity in ordered assemblies, such as organic crystals and co-crystals, to promote RTP by suppressing large-amplitude vibrations, and collisions with host molecules, (as those present in fluid medium), which could contribute to the non-radiative decay of the triplet state, and also probably reducing the permeability to oxygen under ambient conditions. This facilitates potential commercial use of these systems as no film encapsulation is necessary.

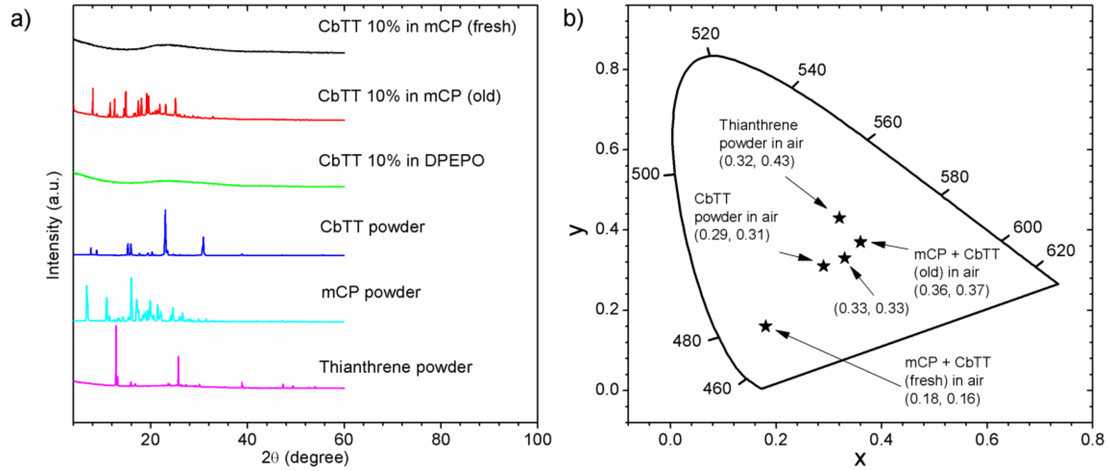

Figure 2. a) XRD diffractograms of investigated powders and films; b) CIE1931 diagram showing color coordinates of investigated solid state samples.

2.3 Photophysical study of crystalline powders

The emission from the solid powders was collected from the compounds as obtained, i.e. in the form of crystalline powders (see **Figure 2 a**). Interestingly, the photoluminescence of **CbTT** and thianthrene in the crystal forms is significantly different than in solution (see **Figure 3**). However, both compounds show blue fluorescence, similarly to that observed in MCH solutions, and also relatively strong room temperature phosphorescence, in the presence of air. **CbTT** clearly shows dual fluorescence-phosphorescence emission, whereas thianthrene, due to dominating contribution of triplet emission is nearly purely phosphorescent. Therefore, the **CbTT** powder shows photoluminescence which is closer to white. The excitation spectra of both crystals show that the absorption in the crystals is different than that of isolated molecules in solution (compare **Figure 3** with **Figure 1**). Both powders can be excited with light up to 400 nm, i.e. at much longer wavelengths than the excitation region that is available in solution – this suggests the existence of aggregates in both crystal forms.

Four emission maxima can be indicated in the photoluminescence of the **CbTT** powder, λ_{max} = 407, 426 nm in fluorescence and λ_{max} = 526, 553 nm in the phosphorescence. On the other hand, the photoluminescence of thianthrene crystals is less complex, and only one maximum λ_{max} = 533 nm is observed. From the properties presented here it is concluded that **CbTT** and thianthrene clearly show aggregation induced phosphorescence emission properties. The observation of aggregation induced luminescence is well known to be due to suppression of large-amplitude rotations in the molecular structure due to the interaction with molecular neighbors. Aggregation induced emission is usually reported on fluorescence, i.e. affecting emission from the singlet state. However, we believe the same is happening here. The transition between the triplet and the ground singlet state is forbidden by spin. This makes the intrinsic decay rate of the triplet state slower than the singlet state, and thus more susceptible to be affected by quenching processes such as collisions with host molecules and oxygen molecules, has it often happens in solution. Additionally, the triplet state is also at lower energy than the singlet state, which according with the golden rule for radiationtless transitions contributes to enhance luminescence quenching, because the non-radiative decay rate of electronic excited states increases as the energy gap decreases, since coupling with higher vibrational levels of the ground state, associated with large-amplitude molecular movements, is enhanced. All these factors are strongly suppressed in solid rigid medium, such as in the crystalline powder and amorphous films studied here, which strongly limit large-amplitude motions, and collisional quenching with host molecules. Therefore, the radiative decay rate from the triplet state is able to compete with non-radiative decay processes and phosphorescence is observed.

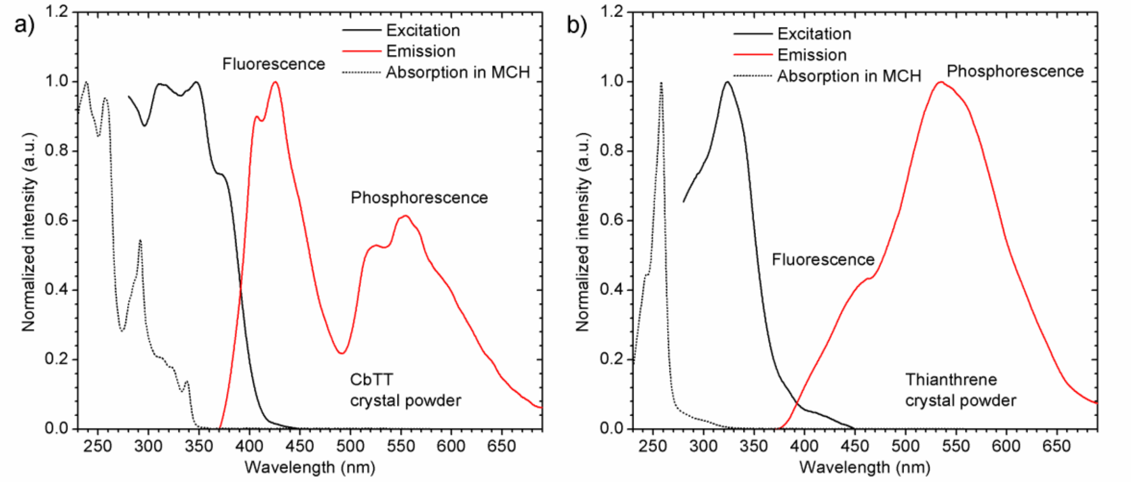

Figure 3. Photoluminescence and excitation spectra of crystalline powders in air.

Time-resolved photoluminescence studies of these powders reveal a complex behavior in both compounds. It is however interesting that both powders behave similarly. Three components are identified in photoluminescence decay: prompt and delayed fluorescence and phosphorescence (**Figure 4**). Indeed a similar observation was previously reported for thianthrene crystals,[34] but not fully explained. In **thianthrene** the prompt fluorescence decays with τ_{PF1} = 2.3 ± 0.1 ns, and τ_{PF2} = 8.2 ± 0.5 ns, followed by delayed fluorescence decaying with τ_{DF1} = 160 ± 20 ns, and τ_{DF2} = 15 ± 3 μs. Finally, at longer times the phosphorescence decay is observed with τ_{PH} = 12 ± 5 ms. In **CbTT** the fluorescence decays with time constants equal to τ_{PF} = 6.3 ± 0.5 ns, due to prompt fluorescence, and τ_{DF1} = 0.20 ± 0.02 μs, and τ_{DF2} = 1.4 ± 0.1 μs, due to delayed fluorescence, and finally the phosphorescence decaying with τ_{PH1} = 6 ± 1 ms, and τ_{PH2} = 23 ± 4 ms, respectively.

In both cases, the spectra associated with the delayed fluorescence diverge from the prompt fluorescence, showing significant spectral shift. This suggests the existence of two different populations of excited states in the powder form, probably due to the presence of different conformers or aggregates. In the case of **CbTT** the delayed fluorescence appears at relatively higher energy than the prompt fluorescence (**Figure 4 c**). This is in contrast with the delayed fluorescence of thianthrene, which appears at slightly lower energy than the prompt fluorescence (**Figure 4 d**). The most probable reasons why the delayed fluorescence in the crystal forms appears at different energies than the prompt fluorescence are possible changes in the geometry of the excited states involved, either between the singlet and triplet states themselves or between the populations of conformers and/or aggregates. The delayed fluorescence, regardless of the mechanism by which it is created, (i.e. TTA or TADF), is originated from the triplet state, and may be strongly affected by conformation, and aggregation. The efficiency of TTA, for example, is controlled by triplet-triplet encounters, which are facilitated in aggregates, and the TADF efficiency is known to vary largely with molecular conformation. Therefore, whereas one of the populations may be able to give origin to strong delayed fluorescence, the other might be inactive in regard of TADF or TTA. This is especially possible in the rigid, densely-packed, environment in the crystal. We should therefore not be surprised by the observation of slightly different emission spectra between prompt and delayed fluorescences.

It is also worthy of notice that the delayed fluorescence of thianthrene is a first order process. This is indicated by the power-dependence experiment (**Figure S3**), thus it can be assigned to a thermally activated delayed fluorescence mechanism (TADF).[35] In contrast, the delayed fluorescence in **CbTT** shows mixed contributions of TADF and triplet-triplet annihilation (TTA). Note however, that the observation of relatively fast TADF in thianthrene, material with S-T gap of ca. 0.4 eV is rather unusual.[7]

Remarkably, as already mentioned, the two powders show prompt and delayed fluorescences, and phosphorescence at room temperature in air. Besides the effect of suppressing luminescence quenching due to collisions with host molecules and large-amplitude vibrations, the two crystalline powders also form a low permeability environment to oxygen, which allows the phosphorescence rate to be able to compete with the quenching rate of the triplet population by oxygen. In the case of thianthrene, whose crystals are larger, there is virtually no effect of oxygen on the emission (**Figure S1**). However, in the case of **CbTT** the effect of oxygen on the emission intensity is noticeable upon degassing the sample, which suggests some degree of oxygen quenching, however still insufficient to quench the phosphorescence completely. Both, the steady state spectra (**Figure S1**) and the time-resolved emission decays (**Figure S2**) show less delayed fluorescence, but more phosphorescence emissions in vacuum than in air. This shows that the direct triplet decay to the ground-state (phosphorescence) is more affected by oxygen than the delayed fluorescence, which involves relatively faster reverse intersystem crossing, and thus is less prone to quenching due to slow oxygen diffusion.

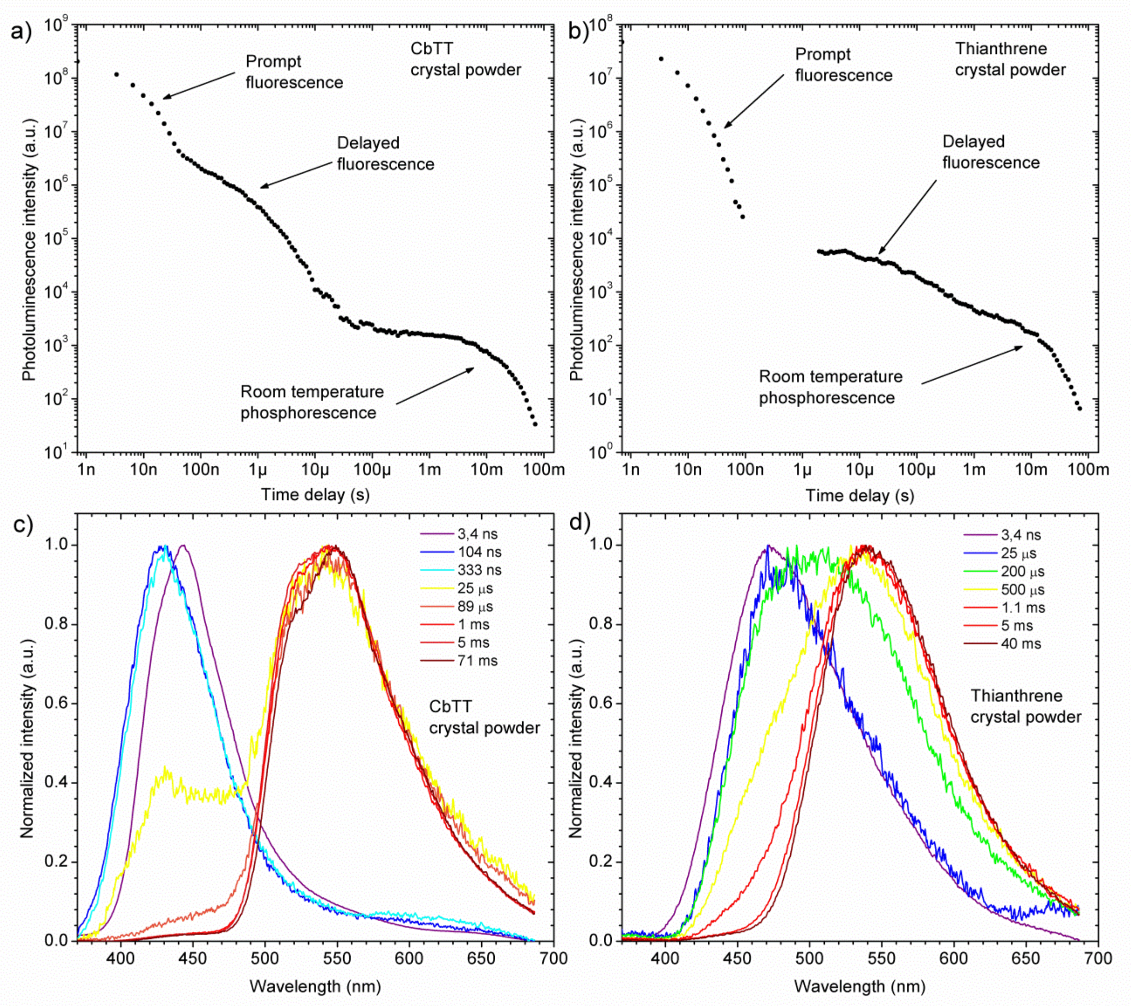

Figure 4. Time-resolved photoluminescence study of crystalline powders at room temperature in the presence of air. a) Photoluminescence decay of **CbTT** powder in air; b) photoluminescence decay of thianthrene powder in air; c) time-resolved spectra of **CbTT** powder in air; d) time-resolved spectra of thianthrene powder in air.

2.4 Photophysical study of CbTT blends

The luminescence from **CbTT** dispersed in different organic matrices is discussed in this section. This study was performed to find an optimal matrix to observe room temperature phosphorescence of the studied thianthrene derivative. Three different blends of **CbTT** were investigated: 1% in zeonex polymer matrix, 10% in **DPEPO**, and 10% in **mCP**. The high doping ratio (10%) was used to quench host emission, **mCP** and **DPEPO**, as by using 1% doping this could disturb the study. The blend with **mCP** was investigated as fresh (new) and as conditioned (old), as previously described. All blends were obtained by drop-cast from toluene solutions at 90˚C (for details see SI). The three blends formed clear, glassy, transparent solid films. The blends were conditioned in ambient conditions for 14 days. After this period it was observed that the films with zeonex or **DPEPO** matrix kept their transparency and photoluminescence properties, in particular only a weak blue fluorescence in the presence of air was observed. However, the film in **mCP** matrix has been found to be cloudy, non-transparent, with a white ivory hue. Interestingly, the photoluminescence changed from weak blue in fresh (new) **mCP/CbTT** film to strong white-greenish luminescence in the old film. This observation suggests that the **CbTT** molecules in the film start to aggregate over time, forming larger domains which strongly scatter visible light, giving an impression of white color. This observation is however a strong indication of crystallization, as it was confirmed by XRD (**Figure 2 a**). This is in clear contrast with **CbTT** films in zeonex and **DPEPO**, which remain amorphous and show no sign of crystallization occurring over time.

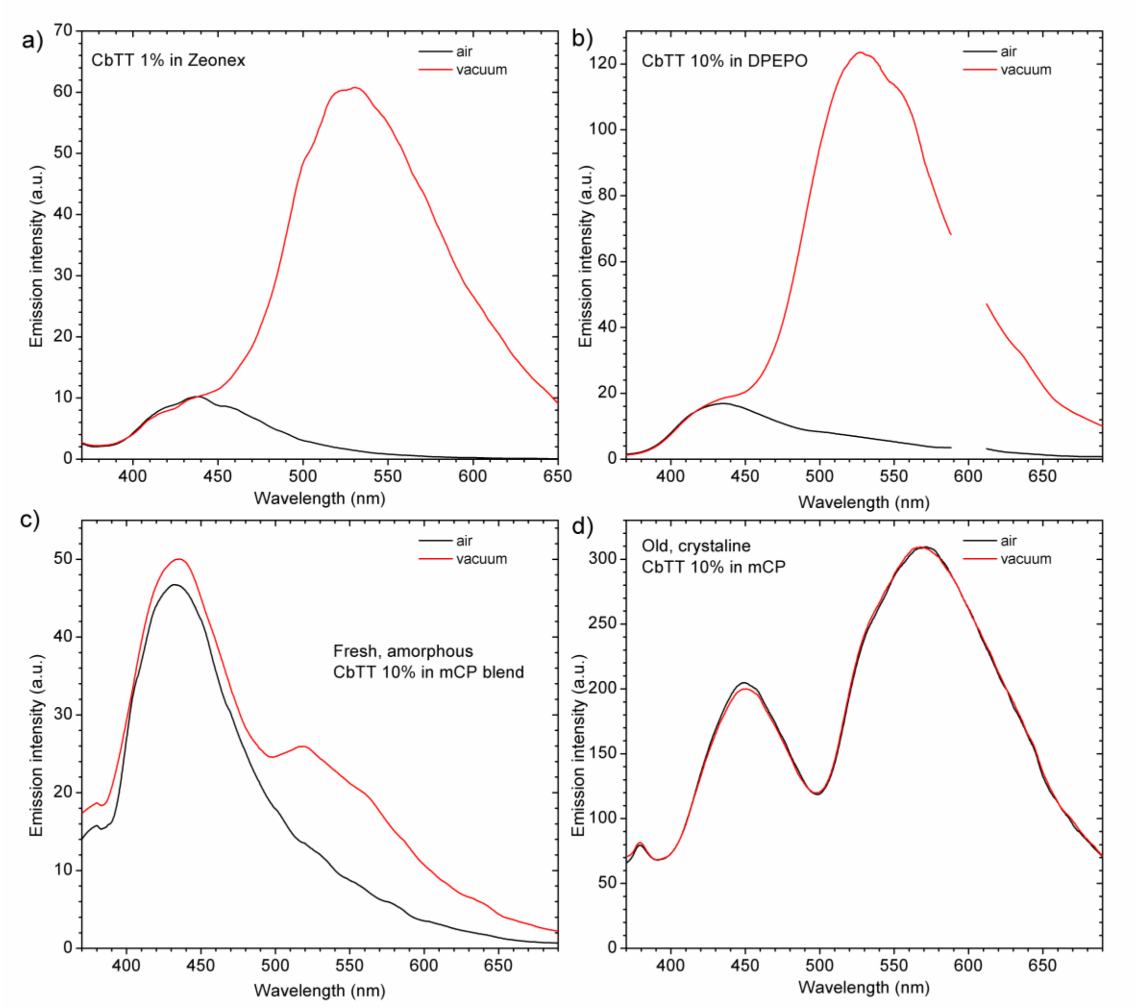

Figure 5. Photoluminescence of **CbTT** blends in different conditions. λ_{max} = 355 nm excitation was used in experiments shown in Figure 5a, 5c, 5d, while emission spectra in Figure 5b were recorded with λ_{max} = 300 nm. Note the second harmonics peak of the excitation beam in Figure 5b (≈600 nm) is not shown for clarity.

Steady-state emission spectra of the investigated blends are presented in **Figure 5**. It is very interesting to note that the photoluminescence behavior of **CbTT** in both zeonex and **DPEPO** is very similar. In both cases showing relatively weak fluorescence in the presence of air, and strong broad phosphorescence in vacuum. Whereas, the phosphorescence lifetime is not identical, it is very similar in both hosts (**Table 1**). Even the phosphorescence spectra are nearly identical in both samples (**Figure 5**). This shows that in hosts of different polarity, non-polar zeonex and polar **DPEPO**[36], the behavior of **CbTT** is very similar (if not identical). On the other hand, the fresh (new) blend with **mCP** shows much smaller contribution of phosphorescence under vacuum, and the phosphorescence is shifted to the red region, being similar to the phosphorescence of the crystalline **CbTT** powder (**Figure 6 b**). Additionally, the lifetime of phosphorescence is here much shorter than in the crystalline state observed in powders, suggesting more effective non-radiative decay than in the powder form. However, the similarity of the phosphorescence spectra of **CbTT** in mCP and in powder form also suggests that the weak phosphorescence may be originated from small crystallites of **CbTT** dispersed in the **mCP** matrix, rather than from a blend or co-crystal. These crystallites however, due to their small size, show larger oxygen permeability, thus their emission is effectively quenched by air. The crystallites are however too small and only account for a trace amount in the sample, and are thus not visible in XRD studies. Interestingly, the prompt fluorescence spectra are not that much affected by the host, all being similar in different environments. In contrast, the thianthrene prompt fluorescence and room temperature phosphorescence are different in zeonex and crystalline powder, as both are red-shifted in the crystalline state (see **Figure 6 c**).

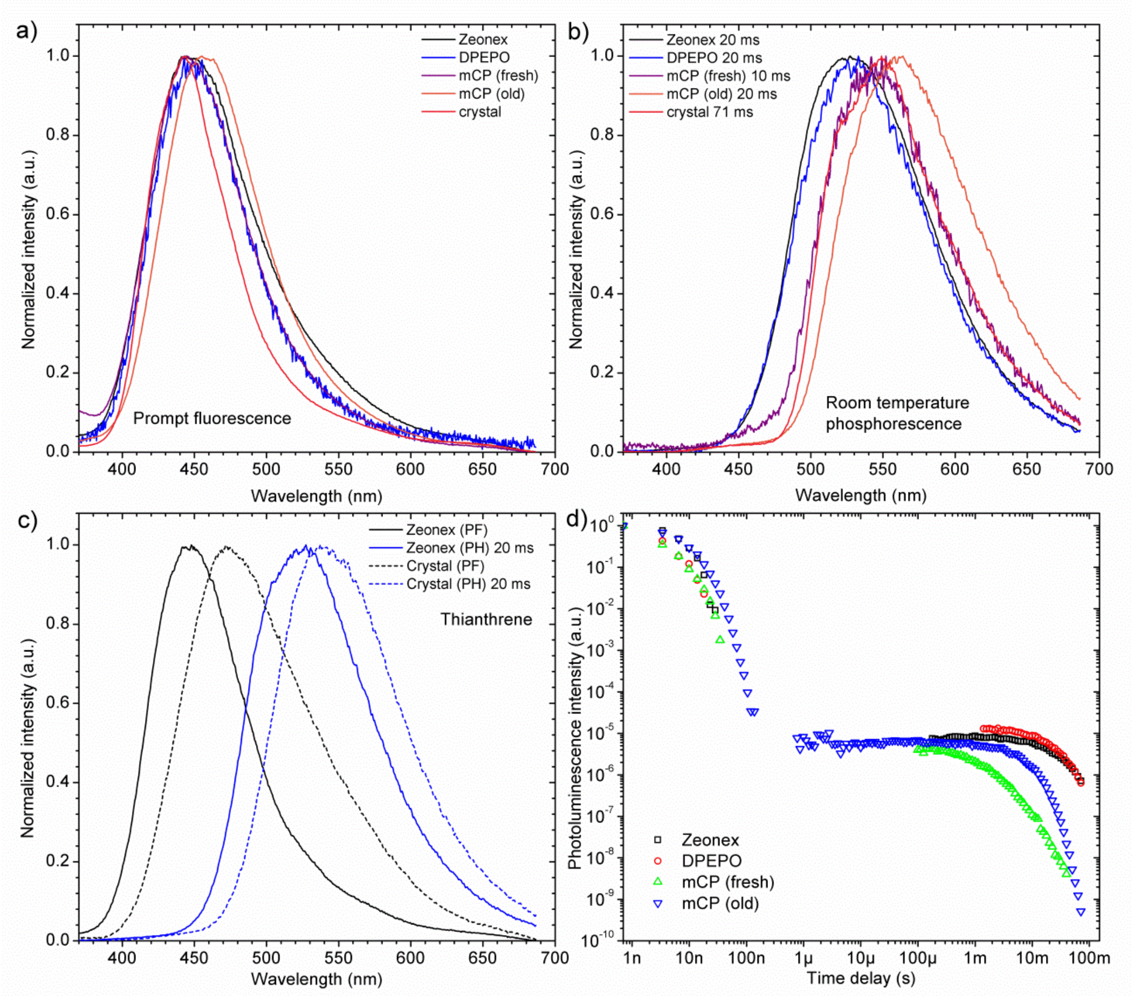

Figure 6. a) Prompt fluorescence (PF) and b) phosphorescence (PH) spectra of **CbTT** in different environments recorded at room temperature. c) Prompt fluorescence and phosphorescence spectra of thianthrene crystals and doped in zeonex matrix. d) Time-resolved decay of **CbTT** in different matrices. Results referring to crystalline **CbTT** and thianthrene and conditioned **mCP** blend were recorded in air. All results recorded at room temperature.

Remarkably, the photoluminescence of **CbTT/mCP** blend after crystallization (old) is totally different than in the fresh film or in any other matrix or in powder. The main similarity between this blend and the powder is that in both cases dual fluorescence-phosphorescence is observed in the presence of air. In fact, this blend shows no effective oxygen quenching, which again indicates reduced film permeability to oxygen in the crystal form. The crystallized (old) blend **CbTT/mCP** film, therefore, shows strong luminescence with remarkable contribution of room-temperature phosphorescence, with a total photoluminescence yield (Φ_{PL}) of 30%, and in the presence of air, whereas the fresh film shows only Φ_{PL} ≈10%. Very close Φ_{PL} ≈ 30% value is observed in zeonex, however only when oxygen is removed. It is also very interesting that **CbTT** is not affected by the host polarity (vide zeonex and **DPEPO**), yet affected by host crystallinity (vide **mCP**). The phosphorescence spectrum in crystal **CbTT/mCP** film is even more red-shifted than in **CbTT** crystals. All these observations suggest that the **CbTT** molecule clearly shows aggregation induced phosphorescence and aggregation enhanced emission,[37] as the quantum yield increases in solid state due to the aggregation of **CbTT** molecules (note the photoluminescence quantum yield in solution Φ_{PL} = 0.04).

In the case of **CbTT** blends, the host plays a crucial role of creating a rigid environment to reduce triplet population quenching and to facilitate efficient RTP. Zeonex and **DPEPO** also perfectly reduce the quenching of triplet states by strongly limiting large-amplitude motions in the emitter, and collisional quenching with host molecules due to their relatively high glass transition temperature or melting point.[38,39] However, these hosts are highly permeable to oxygen and RTP is entirely quenched in air. On the other hand, the less rigid **mCP** with much lower t_g = 55 °C [40] does not effectively suppress the non-radiative decay of the triplet state, but after crystallization of the **CbTT/mCP** matrix the **CbTT** surroundings become more rigid, and much less permeable to oxygen. These conditions are in favor to facilitate room temperature phosphorescence in the presence of air, which is indeed observed.

Table 1. Spectroscopic characteristics of **CbTT** and **thianthrene** in different environments.

Compound	**Sample form**	**λ_{PL}, nm**[a]	**S_1 / T_1, eV**[b]	**τ_{PF}, ns**[c]	**τ_{PH}, ms**[d]	**Φ_{PL}** [e]
CbTT	MCH solution (10^{-5} M)	435	3.17 / -	9.4 ± 0.4	-	0.04
	1:99 zeonex blend	532	3.18 / 2.69	7.4 ± 0.4	26.5 ± 0.6	0.27
	1:9 DPEPO blend	528	3.10 / 2.71	3.5 ± 0.2	21.6 ± 0.5	-
	1:9 mCP blend (fresh)	435, 518	3.15 / 2.62	5.1 ± 0.2	0.9 ± 0.2 (71%) 4 ± 1 (29%)	0.10
	1:9 mCP blend (old)	450, 570	3.10 / 2.52	8.5 ± 0.1*	6.9 ± 0.2*	0.31*
	crystalline powder	426, 553	3.12 / 2.56	6.3 ± 0.5*	23 ± 4 (53%) 6 ± 1 (47%)*	-
Thianthrene	MCH solution ($5\cdot10^{-5}$ M)	431	3.18 / -	-	-	0.03
	1:99 zeonex blend	535	3.13 / 2.70[1]	11.3 ± 0.6	18 ± 1[1]	-
	crystalline powder	533	3.03 / 2.61	2.3 ± 0.1 (61%) 8.2 ± 0.5 (39%)*	12 ± 5*	-

* Measured in air. The differences in the lifetimes recorded in vacuum were not statistically significant showing no oxygen effect on lifetime. [a] Photoluminescence maxima in vacuum; [b] *Onset* singlet and triplet energy from room temperature spectra in vacuum; [c] Prompt fluorescence lifetime at room temperature in vacuum – please note, the lifetime of delayed fluorescence observed in crystals is not shown here; [d] Phosphorescence lifetime at room temperature in vacuum; [e] Photoluminescence quantum yield at room temperature in oxygen-free conditions. The values present an average error of ± 0.01 for solution measurements and ± 0.05 for solid-state measurements.

3. CONCLUSIONS

A thianthrene derivative was shown to present aggregation induced phosphorescence emission at room temperature, and in the presence of air. These remarkable properties of the **CbTT** crystalline powder and of **CbTT/mCP** blend were investigated and compared with a close photophysical study of the parent compound thianthrene. The room-temperature phosphorescence and dual fluorescence-phosphorescence emission of **CbTT** show air-resistant phosphorescence when dispersed in the **mCP** host, after crystallization, and in the powder form. However, when **CbTT** is dispersed in zeonex and **DPEPO** no crystalization occurs and the room-temperature phosphorescence is completely quenched by oxygen. The phosphorescence of the blend can hardly be distinguished by the naked eye, but it is easily distinguished with a detector working with frequency above 30 Hz. Films showing dual fluorescence-phosphorescence at RT in air can be used to produce anti-counterfeiting markers that do not obviously look different from regular fluorescent marks.[21]

ASSOCIATED CONTENT

Supporting Information.

The following files are available free of charge.

Details of experimental methods and film production, additional photophysical results, electrochemistry and density functional theory calculations (PDF)

AUTHOR INFORMATION

Corresponding Author

*E-mail: f.m.b.dias@durham.ac.uk

Author Contributions

P.P. suggested to investigate RTP properties of presented molecules, performed all photophysical and electrochemical measurements, and wrote the manuscript. A.S. synthesized CbTT molecule.

A.L., R.P., and R.T. performed XRD study of powders and films. R.T. recorded DSC thermogram of CbTT. A.K., R.M., and A.S. characterized CbTT molecule to prove its chemical structure. P.S. supervised A.K in her work. D.J. and S.P. supervised R.T. in XRD measurements. P.D. and J.S. supervised A.S. in synthetic work. J.V.G. supervised R.P. in XRD study. P.D. supervised P.P. in electrochemical measurements. F.B.D. supervised P.P. in the photophysical work and writing of the manuscript. The manuscript was written through contributions of all authors. All authors have given approval to the final version of the manuscript.

Notes

The authors declare no competing financial interest.

ACKNOWLEDGMENT

P.P., R.P., and A.K. thank to the European Union for financial support from EU's Horizon 2020 for funding the EXCILIGHT project under grant agreement No. 674990. R.T. acknowledges the EU's Horizon 2020 for funding the ORZEL project under grant agreement No. 691684.

REFERENCES

1 Pander, P.; Swist, A.; Soloducho, J.; Dias, F. B. Room Temperature Phosphorescence Lifetime and Spectrum Tuning of Substituted Thianthrenes. *Dye. Pigment.* **2017**, *142*, 315–322.

2 Liu, H.; Gao, Y.; Cao, J.; Li, T.; Wen, Y.; Ge, Y.; Zhang, L.; Pan, G.; Zhou, T.; Yang, B. Efficient Room-Temperature Phosphorescence Based on a Pure Organic Sulfur-Containing Heterocycle: Folding-Induced Spin–orbit Coupling Enhancement. *Mater.*

Chem. Front. **2018**, *2*, 1853–1858.

3 Pander, P.; Data, P.; Turczyn, R.; Lapkowski, M.; Swist, A.; Soloducho, J.; Monkman, A. P. Synthesis and Characterization of Chalcogenophene-Based Monomers with Pyridine Acceptor Unit. *Electrochim. Acta* **2016**, *210*, 773–782.

4 Pander, P.; Motyka, R.; Zassowski, P.; Lapkowski, M.; Swist, A.; Data, P. Electrochromic Properties of Novel Selenophene and Tellurophene Derivatives Based on Carbazole and Triphenylamine Core. *J. Phys. Chem. C* **2017**, acs.jpcc.7b00216.

5 Xue, P.; Wang, P.; Chen, P.; Yao, B.; Gong, P.; Sun, J.; Zhang, Z.; Lu, R. Bright Persistent Luminescence from Pure Organic Molecules through a Moderate Intermolecular Heavy Atom Effect. *Chem. Sci.* **2017**, *8*, 6060–6065.

6 Hayduk, M.; Riebe, S.; Voskuhl, J. Phosphorescence Through Hindered Motion of Pure Organic Emitters. *Chem. - A Eur. J.* **2018**, *24*, 12221–12230.

7 Pander, P.; Swist, A.; Motyka, R.; Soloducho, J.; Dias, F. B.; Data, P. Thermally Activated Delayed Fluorescence with a Narrow Emission Spectrum and Organic Room Temperature Phosphorescence by Controlling Spin–orbit Coupling and Phosphorescence Lifetime of Metal-Free Organic Molecules. *J. Mater. Chem. C* **2018**, *6*, 5434–5443.

8 Wróblowska, M.; Kudelko, A.; Kuźnik, N.; Łaba, K.; Łapkowski, M. Synthesis of Extended 1,3,4-Oxadiazole and 1,3,4-Thiadiazole Derivatives in the Suzuki Cross-Coupling Reactions. *J. Heterocycl. Chem.* **2017**, *54*, 1550–1557.

9 Joule, J. A. Thianthrenes. In *Advances in Heterocyclic Chemistry*; 1990; Vol. 48, pp 301–393.

10 Laba, K.; Data, P.; Zassowski, P.; Pander, P.; Lapkowski, M.; Pluta, K.; Monkman, A. P. Diquinoline Derivatives as Materials for Potential Optoelectronic Applications. *J. Phys. Chem. C* **2015**, *119*, 13129–13137.

11 Ward, J. S.; Nobuyasu, R. S.; Batsanov, A. S.; Data, P.; Monkman, A. P.; Dias, F. B.; Bryce, M. R. The Interplay of Thermally Activated Delayed Fluorescence (TADF) and Room Temperature Organic Phosphorescence in Sterically-Constrained Donor–acceptor Charge-Transfer Molecules. *Chem. Commun.* **2016**, *52*, 3–6.

12 Kabe, R.; Adachi, C. Organic Long Persistent Luminescence. *Nature* **2017**, *550*, 384–387.

13 Hirata, S.; Totani, K.; Zhang, J.; Yamashita, T.; Kaji, H.; Marder, S. R.; Watanabe, T.; Adachi, C. Efficient Persistent Room Temperature Phosphorescence in Organic Amorphous Materials under Ambient Conditions. *Adv. Funct. Mater.* **2013**, *23*, 3386–3397.

14 Huang, R.; Avó, J.; Northey, T.; Chaning-Pearce, E.; dos Santos, P. L.; Ward, J. S.; Data, P.; Etherington, M. K.; Fox, M. A.; Penfold, T. J.; Berberan-Santos, M. N.; Lima, J. C.; Bryce, M. R.; Dias, F. B. The Contributions of Molecular Vibrations and Higher Triplet Levels to the Intersystem Crossing Mechanism in Metal-Free Organic Emitters. *J. Mater. Chem. C* **2017**, *5*, 6269–6280.

15 Ward, J. S.; Nobuyasu, R. S.; Batsanov, A. S.; Data, P.; Monkman, A. P.; Dias, F. B.; Bryce, M. R. The Interplay of Thermally Activated Delayed Fluorescence (TADF) and Room Temperature Organic Phosphorescence in Sterically-Constrained Donor–acceptor Charge-Transfer Molecules. *Chem. Commun.* **2016**, *52*, 3–6.

16 Bolton, O.; Lee, K.; Kim, H.-J.; Lin, K. Y.; Kim, J. Activating Efficient Phosphorescence from Purely Organic Materials by Crystal Design. *Nat. Chem.* **2011**, *3*, 205–210.

17 Chateau, D.; Chaput, F.; Lopes, C.; Lindgren, M.; Brännlund, C.; Öhgren, J.; Djourelov, N.; Nedelec, P.; Desroches, C.; Eliasson, B.; Kindahl, T.; Lerouge, F.; Andraud, C.; Parola, S. Silica Hybrid Sol–Gel Materials with Unusually High Concentration of Pt–Organic Molecular Guests: Studies of Luminescence and Nonlinear Absorption of Light. *ACS Appl. Mater. Interfaces* **2012**, *4*, 2369–2377.

18 Dias, F. B.; Bourdakos, K. N.; Jankus, V.; Moss, K. C.; Kamtekar, K. T.; Bhalla, V.; Santos, J.; Bryce, M. R.; Monkman, A. P. Triplet Harvesting with 100% Efficiency by Way of Thermally Activated Delayed Fluorescence in Charge Transfer OLED Emitters. *Adv. Mater.* **2013**, *25*, 3707–3714.

19 Data, P.; Pander, P.; Okazaki, M.; Takeda, Y.; Minakata, S.; Monkman, A. P. Dibenzo[A,j]Phenazine-Cored Donor-Acceptor-Donor Compounds as Green-to-Red/NIR Thermally Activated Delayed Fluorescence Organic Light Emitters. *Angew. Chemie Int. Ed.* **2016**, *55*, 5739–5744.

20 Xu, B.; Wu, H.; Chen, J.; Yang, Z.; Yang, Z.; Wu, Y.-C.; Zhang, Y.; Jin, C.; Lu, P.-Y.; Chi, Z.; Liu, S.; Xu, J.; Aldred, M. White-Light Emission from a Single Heavy Atom-Free Molecule with Room Temperature Phosphorescence, Mechanochromism and Thermochromism. *Chem. Sci.* **2017**, *8*, 1909–1914.

21 Jiang, K.; Zhang, L.; Lu, J.; Xu, C.; Cai, C.; Lin, H. Triple-Mode Emission of Carbon Dots: Applications for Advanced Anti-Counterfeiting. *Angew. Chemie - Int. Ed.* **2016**, *55*, 7231–7235.

22 Pander, P.; Swist, A.; Zassowski, P.; Soloducho, J.; Lapkowski, M.; Data, P. Electrochemistry and Spectroelectrochemistry of Polymers Based on D-A-D and D-D-D Bis(N -Carbazolyl) Monomers, Effect of the Donor/acceptor Core on Their Properties. *Electrochim. Acta* **2017**, *257*, 192–202.

23 Moss, K. C.; Bourdakos, K. N.; Bhalla, V.; Kamtekar, K. T.; Bryce, M. R.; Fox, M. A.; Vaughan, H. L.; Dias, F. B.; Monkman, A. P. Tuning the Intramolecular Charge Transfer Emission from Deep Blue to Green in Ambipolar Systems Based on Dibenzothiophene S , S -Dioxide by Manipulation of Conjugation and Strength of the Electron Donor Units. *J. Org. Chem.* **2010**, *75*, 6771–6781.

24 Uoyama, H.; Goushi, K.; Shizu, K.; Nomura, H.; Adachi, C. Highly Efficient Organic Light-Emitting Diodes from Delayed Fluorescence. *Nature* **2012**, *492*, 234–238.

25 Data, P.; Motyka, R.; Lapkowski, M.; Suwinski, J.; Monkman, A. P. Spectroelectrochemical Analysis of Charge Carriers as a Way of Improving Poly(p-Phenylene)-Based Electrochromic Windows. *J. Phys. Chem. C* **2015**, *119*, 20188–20200.

26 Data, P.; Pander, P.; Zassowski, P.; Mimaite, V.; Karon, K.; Lapkowski, M.; Grazulevicius, J. V.; Slepski, P.; Darowicki, K. Electrochemically Induced Synthesis of Triphenylamine-Based Polyhydrazones. *Electrochim. Acta* **2017**, *230*, 10–21.

27 Iwan, A.; Sek, D. Polymers with Triphenylamine Units: Photonic and Electroactive Materials. *Prog. Polym. Sci.* **2011**, *36*, 1277–1325.

28 Gudeika, D.; Lygaitis, R.; Mimaitė, V.; Grazulevicius, J. V.; Jankauskas, V.; Lapkowski, M.; Data, P. Hydrazones Containing Electron-Accepting and Electron-Donating Moieties.

Dye. Pigment. **2011**, *91*, 13–19.

29 Karon, K.; Lapkowski, M.; Dabuliene, A.; Tomkeviciene, A.; Kostiv, N.; Grazulevicius, J. V. Spectroelectrochemical Characterization of Conducting Polymers from Star-Shaped Carbazole-Triphenylamine Compounds. *Electrochim. Acta* **2015**, *154*, 119–127.

30 Beck, J.; Bredow, T.; Tjahjanto, R. T. Thianthrene Radical Cation Hexafluorophosphate. *Zeitschrift fur Naturforsch. - Sect. B J. Chem. Sci.* **2009**, *64*, 145–152.

31 Świst, A.; Sołoducho, J.; Data, P.; Łapkowski, M. Thianthrene-Based Oligomers as Hole Transporting Materials. *Arkivoc* **2012**, *2012*, 193–209.

32 Pereira, D.; Pinto, A.; Califórnia, A.; Gomes, J.; Pereira, L. Control of a White Organic Light Emitting Diode Emission Parameters Using a Single Doped RGB Active Layer. *Mater. Sci. Eng. B* **2016**, *211*, 156–165.

33 Pereira, D. D. S.; dos Santos, P. L.; Ward, J. S.; Data, P.; Okazaki, M.; Takeda, Y.; Minakata, S.; Bryce, M. R.; Monkman, A. P. An Optical and Electrical Study of Full Thermally Activated Delayed Fluorescent White Organic Light-Emitting Diodes. *Sci. Rep.* **2017**, *7*, 6234.

34 Arena, A.; Campagna, S.; Mezzasalma, A. M.; Saija, R.; Saitta, G. Analysis of the Phosphorescence of Thianthren Crystals. *Nuovo Cim. D* **1993**, *15*, 1521–1532.

35 Dias, F. B.; Bourdakos, K. N.; Jankus, V.; Moss, K. C.; Kamtekar, K. T.; Bhalla, V.; Santos, J.; Bryce, M. R.; Monkman, A. P. Triplet Harvesting with 100% Efficiency by Way of Thermally Activated Delayed Fluorescence in Charge Transfer OLED Emitters. *Adv. Mater.* **2013**, *25*, 3707–3714.

36 dos Santos, P. L.; Ward, J. S.; Bryce, M. R.; Monkman, A. P. Using Guest–Host Interactions To Optimize the Efficiency of TADF OLEDs. *J. Phys. Chem. Lett.* **2016**, *7*, 3341–3346.

37 Mei, J.; Leung, N. L. C.; Kwok, R. T. K.; Lam, J. W. Y.; Tang, B. Z. Aggregation-Induced Emission: Together We Shine, United We Soar! *Chem. Rev.* **2015**, *115*, 11718–11940.

38 Han, C.; Zhao, Y.; Xu, H.; Chen, J.; Deng, Z.; Ma, D.; Li, Q.; Yan, P. A Simple Phosphine-Oxide Host with a Multi-Insulating Structure: High Triplet Energy Level for Efficient Blue Electrophosphorescence. *Chem. - A Eur. J.* **2011**, *17*, 5800–5803.

39 Zeonex catalogue http://www.zeon.co.jp/content/200181690.pdf (accessed Aug 15, 2018).

40 Gong, M.; Cha, J.; Lee, C. W. Synthesis and Device Properties of mCP Analogues Based on Fused-Ring Carbazole Moiety. *Org. Electron.* **2017**, *42*, 66–74.

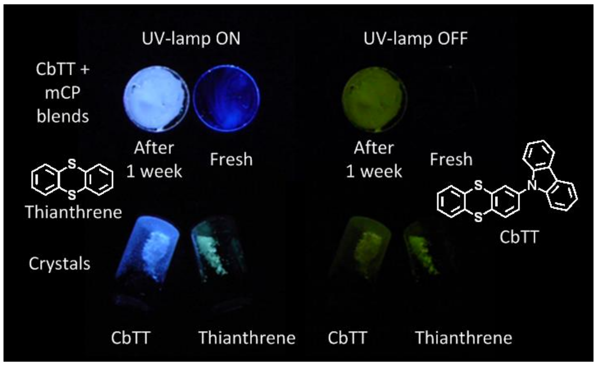
UV-lamp ON
UV-lamp OFF
CbTT +
mCP
blends
After
1 week
Fresh
After
1 week
Fresh
S
S
Thianthrene
S
S
N
CbTT
Crystals
CbTT
Thianthrene
CbTT
Thianthrene